



A 5000-year paleoclimate record from Nettilling Lake (Baffin Island) based on diatom assemblages and oxygen isotope composition

BILJANA NARANCIC,^{1,2*}  ÉMILIE SAULNIER-TALBOT,²  HANNO MEYER¹  and REINHARD PIENITZ² 

¹Alfred Wegener Institute (AWI) Helmholtz Centre for Polar and Marine Research, Research Unit Potsdam, Potsdam, Germany

²Laboratoire de Paléoécologie Aquatique, Centre d'études nordiques (CEN) & Département de Géographie, Université Laval, Québec, QC, Canada

Received 29 April 2021; Revised 3 July 2021; Accepted 4 August 2021

ABSTRACT: Sedimentary diatoms have been used to quantitatively reconstruct climate-related variables, such as temperature at different timescales. Even though temperature is often less of a key driver of diatom ecology than other environmental parameters (water chemistry), diatom inference models have been shown to be reliable in deducing past temperature trends. In addition, the oxygen isotope composition ($\delta^{18}\text{O}_{\text{diatom}}$) preserved in buried diatom frustules has demonstrated its potential to reflect climatic and hydrological conditions at the time of frustule formation. This study combines results from both diatom-based climate proxies to reconstruct summer water and mean annual air temperatures, and hydrological trends in Nettilling Lake, Baffin Island, from ca. 5000 to 500 cal a BP. Diatom-inferred temperatures revealed an overall ca. 2 °C cooling throughout the Late-Holocene. The $\delta^{18}\text{O}_{\text{diatom}}$ values showed an increasing trend up to ca. 1900 cal a BP, where they reached their highest values (+24.8‰ at 15 cm) and thereafter decreased to their lowest values (+21.4‰ at 4 cm). These trends were linked to meltwater inflows associated with Penny Ice Cap thaw rate that was in turn controlled by regional climatic conditions which went from intensified cooling during the Neoglacial period to slight warming thereafter. Our results suggest that diatom- and diatom-isotope-based temperature and hydrological reconstructions can identify trends related to the natural climate system variability. The diatom oxygen isotopes are useful for paleoenvironmental studies of terrestrial aquatic ecosystems, but not for all hydrological systems are the ideal temperature proxy. Hence, the combination of proxies helps to disentangle temperature and hydrological effects for paleoclimatic reconstructions and may support future studies of postglacial environmental change in northern lakes. © 2021 John Wiley & Sons, Ltd.

KEYWORDS: diatoms; hydroclimate; Nettilling Lake; oxygen isotopes; temperature

Introduction

High-quality paleoclimatic data are necessary to better understand the long-term dynamics in various components of the Earth's climate system and are required to validate climate prediction models. Lakes are integrated systems of environmental change that incorporate interactions between the geosphere, hydrosphere, atmosphere and biosphere. They are common features of northern landscapes, owing to the regional glacial history. Northern lakes are remote and usually pristine and as such offer a unique setting, deprived from direct human impact, for studying long-term environmental change. Their sedimentary archives provide detailed information on past environmental variability in their basins and catchments (Saulnier-Talbot, 2016). The biological remains preserved in lake sediments are routinely used to infer past fluctuations of multiple environmental variables (Smol *et al.*, 2001).

Diatoms are single-celled photosynthetic organisms with a hydrated silica 'shell' (frustule). They are ubiquitous in all aquatic environments, and are one of the most commonly used groups of bio-indicators in lake sediments. Their abundance, diversity and excellent preservation in sediments, combined with their sensitivity to environmental variables, make them a preferred proxy in many Late Quaternary studies (Palagushkina *et al.*, 2017; Huang *et al.*, 2020). Therefore, paleoecological

inferences are based on their current ecological preferences. Diatoms have been used to infer past changes in lake water chemistry (Jacques *et al.*, 2016), salinity (Narancic *et al.*, 2016), nutrient concentrations (Rodríguez-Alcalá *et al.*, 2020), water depth (Gushulak *et al.*, 2017) and climate (Rühland *et al.*, 2015). Several studies have used diatoms to reconstruct past temperature from sediment records using transfer functions (Pienitz *et al.*, 1995; Joynt and Wolfe, 2001; Rühland *et al.*, 2015; Goldenberg Vilar *et al.*, 2018; Reavie and Cai, 2019; Maslennikova, 2020; Sui *et al.*, 2020). Additionally, many physical and chemical variables in lake systems to which diatoms are sensitive (thermal stratification and ice-cover) are closely linked to changes in temperature. However, to separate the specific influence of temperature changes on diatom assemblage composition from other variables remains a challenge.

In previous studies on Baffin Island in Arctic Canada, lacustrine proxies yielded an Early-Holocene warm period (ca. 10 000–4000 cal a BP) that was interrupted by short, cold reversals between 9500 and 8000 cal a BP (Crump *et al.*, 2020), followed by Neoglacial cooling (ca. 6000 BP; McKay *et al.*, 2018) that culminated during the Little Ice Age (675 BP; Miller *et al.*, 2012). Joynt and Wolfe (2001) developed a diatom-based quantitative inference model from sedimentary assemblages collected in lakes located throughout eastern Baffin Island, and were able to reconstruct summer water temperatures covering the past 5000 cal a BP from sediment records preserved in Fog lake, on Baffin's eastern coast. Their results generally agreed with other

*Correspondence: B. Narancic, as above.
E-mail: biljana.narancic.1@ulaval.ca

independent paleoclimatic reconstructions for this region (Briner *et al.*, 2016).

Biogenic silica ($\text{SiO}_2 \cdot n\text{H}_2\text{O}$) is produced within the diatom cells and incorporated in the frustules through the process of biogenesis (i.e. the transformation of dissolved silicate to particulate skeletal material). The oxygen isotope composition of diatom biogenic silica ($\delta^{18}\text{O}_{\text{diatom}}$) has proven to be a useful paleoclimatic indicator that reflects the lake water temperature and the oxygen isotope composition of the water in which it was formed (Leng and Barker, 2006) with very small effects of post-depositional processes (e.g. diagenesis) over time (Dodd *et al.*, 2012). Sample contamination assessment by clay/mineral particles (excluding aluminum oxide Al_2O_3) allows for a reliable correction technique as described by Chaplignin *et al.* (2012). $\delta^{18}\text{O}_{\text{diatom}}$ has been used in numerous studies as an alternative to more traditional $\delta^{18}\text{O}_{\text{carbonate}}$ analyses, especially in the polar regions where carbonates are less abundant and it has proven to be a reliable paleoclimate indicator (Juillet-Leclerc and Labeyrie, 1987; Quesada *et al.*, 2015; Bailey *et al.*, 2018; Swann *et al.*, 2018; Cartier *et al.*, 2019; Kostrova *et al.*, 2019).

The aim of this study was to assess the consistency in paleoclimatic inferences obtained from downcore diatom assemblages and from the oxygen isotopic signal preserved in diatom biogenic silica. Using sediments from Nettilling Lake (Baffin Island), we reconstructed summer surface water temperature (SWT) and mean annual air temperature (MAAT) for the past ca. 5000 cal a BP using downcore diatom assemblage composition by applying the Joynt and Wolfe (2001) model and compared the outcome to hydroclimatic changes associated with temperature changes using $\delta^{18}\text{O}_{\text{diatom}}$. This combination of biological and geochemical proxies from the same sedimentary material provides a unique opportunity to assess their coherence in climatic reconstructions.

Materials and methods

Study site and sediment core sampling

Nettilling Lake is the largest lake in the Canadian Arctic Archipelago. It is located in the Great Plain of the Koukdjuak on Baffin Island, Nunavut (Fig. 1; $66^\circ 21.3082' \text{N}$, $70^\circ 16.1133' \text{W}$). Its early postglacial history is well documented (Beaudoin *et al.*, 2016; Chaplignin *et al.*, 2016; Narancic *et al.*, 2016). In the early postglacial period, the region was submerged by the postglacial Tyrrell Sea due to glacio-isostatic depression exerted by the Laurentide Ice Sheet (LIS). Narancic *et al.* (2016) showed that the Nettilling Lake basin experienced a relatively rapid and uniform marine invasion during the Early Holocene (ca. 8000 cal a BP), followed by progressive freshening until ca. 5000 cal a BP when limnological conditions were established.

The lake basin is divided into the western lowlands of Paleozoic carbonates, and the eastern low relief of Precambrian granite/gneiss plateaus. An important plume of suspended particulate matter, situated in the north-eastern sector of the lake, is formed by the inflow of meltwaters from the Penny Ice Cap (PIC) via the Isurtuq River. Beaudoin *et al.* (2016) analyzed a sediment core taken close to the Isurtuq River inflow and found evidence of hydroclimatic connectivity between accelerated sedimentation rates and summer melt rates of the PIC since the Little Ice Age.

The coring site ($66^\circ 34.294' \text{N}$, $70^\circ 06.565' \text{W}$) is located in the Precambrian, eastern sector of the basin, within the lake's plume region (Fig. 1 and Supporting Information Fig. S1). This plume location was preferred because of the apparent influence of Penny ice melt signal and rather distal position (12 km away)

from the river mouth, avoiding potential sediment disturbance. The 82-cm-long Ni-2B core was extracted from ca. 14 m water depth using a percussion corer in spring 2012, while the lake was still covered with >1-m-thick ice. The core was preserved intact using Zorbitrol to minimize movement during transport and split horizontally into halves once in the laboratory. One half was fitted with a u-channel sampler for paleomagnetic measurements, while the other was subsampled at 0.5-cm intervals for diatom taxonomy and oxygen isotopic analyses. Here, we present the top 35 cm of the core, which correspond to the last ca. 5000 years of sedimentary history.

At the coring site, punctual Secchi depth (ca. 55 cm) and surface and bottom water temperature (7.5°C for both) were measured during a midsummer expedition in 2014 with a YSI profiler (600-Q Multi Parameter Water Quality Monitor), indicating a well-mixed and nutrient-poor lake. Chaplignin *et al.* (2016) partitioned the contribution of Nettilling Lake's main tributaries through isotopic hydrology and hydrochemical data. They found that the Amadjuak River, which drains Amadjuak Lake to the south, and the Isurtuq River in the north-east presently contribute 43 and 57% to the lake's water volume, respectively, assuming Nettilling Lake as a two-component mixture of these two major inflows. Narancic *et al.* (2021) reconstructed slightly alkaline lake water pH, ranging between pH 7.1 and 7.7 for the past 5000 years, by applying a diatom-based inference model. This rather stable lake water chemistry, mainly controlled by PIC meltwater inflows, provides evidence of the usefulness of the site to apply and compare these proxies in paleoreconstructions.

Diatom assemblage analysis

For diatom assemblage analysis, 26 samples of the upper 35 cm of the Ni2-B core were freeze-dried and cleaned using the method of Scherer (1994). Of 26 samples, 16 were already published in Narancic *et al.* (2016) and an additional 10 were added to this study allowing for higher resolution of Nettilling Lake's lacustrine conditions. A few drops of 10% dilute HCl were added to samples to remove the carbonates, followed by 5 ml of 20% H_2O_2 to oxidize organics and disaggregate particles. After several rinsing steps, the siliceous material was left to settle in glass vials in 10 ml of distilled water. The siliceous material was mounted onto glass microscope slides with the synthetic resin Naphrax. At least 300 diatom valves were enumerated along random transects in each sample under oil immersion at a magnification of 1000x using a Zeiss Axioskop 2 light microscope. Identifications were made to the lowest taxonomic level based on different floras, and relative taxon abundance was calculated as the percentage of the total valves counted (taxonomic results are presented in Narancic *et al.*, 2021).

Joynt and Wolfe (2001) applied canonical correspondence analysis using forward selection and Monte Carlo permutation tests to identify variables with significant environmental controls over sedimentary diatom assemblages from a series of 61 lakes spanning a north-south gradient ($62\text{--}74^\circ \text{N}$) across Baffin Island. They then developed predictive models using weighted-averaging regression and calibration for conductivity, pH, SWT and MAAT, collectively accounting for 42.2% of the variance initially explained by the original 16 environmental variables included in the analysis. The SWT and MAAT models have an r^2 of 0.48 and 0.43 and a root mean squared error of prediction of 1.94 and 1.81°C , respectively. Both are slightly biased in the extremes of their respective gradients. This statistical performance suggests these are slightly less robust than other diatom-based temperature transfer functions, but nevertheless significant. The transfer function was applied to our downcore diatom data using the C2 software (Juggins, 2013). The downcore assemblage data were fit to the

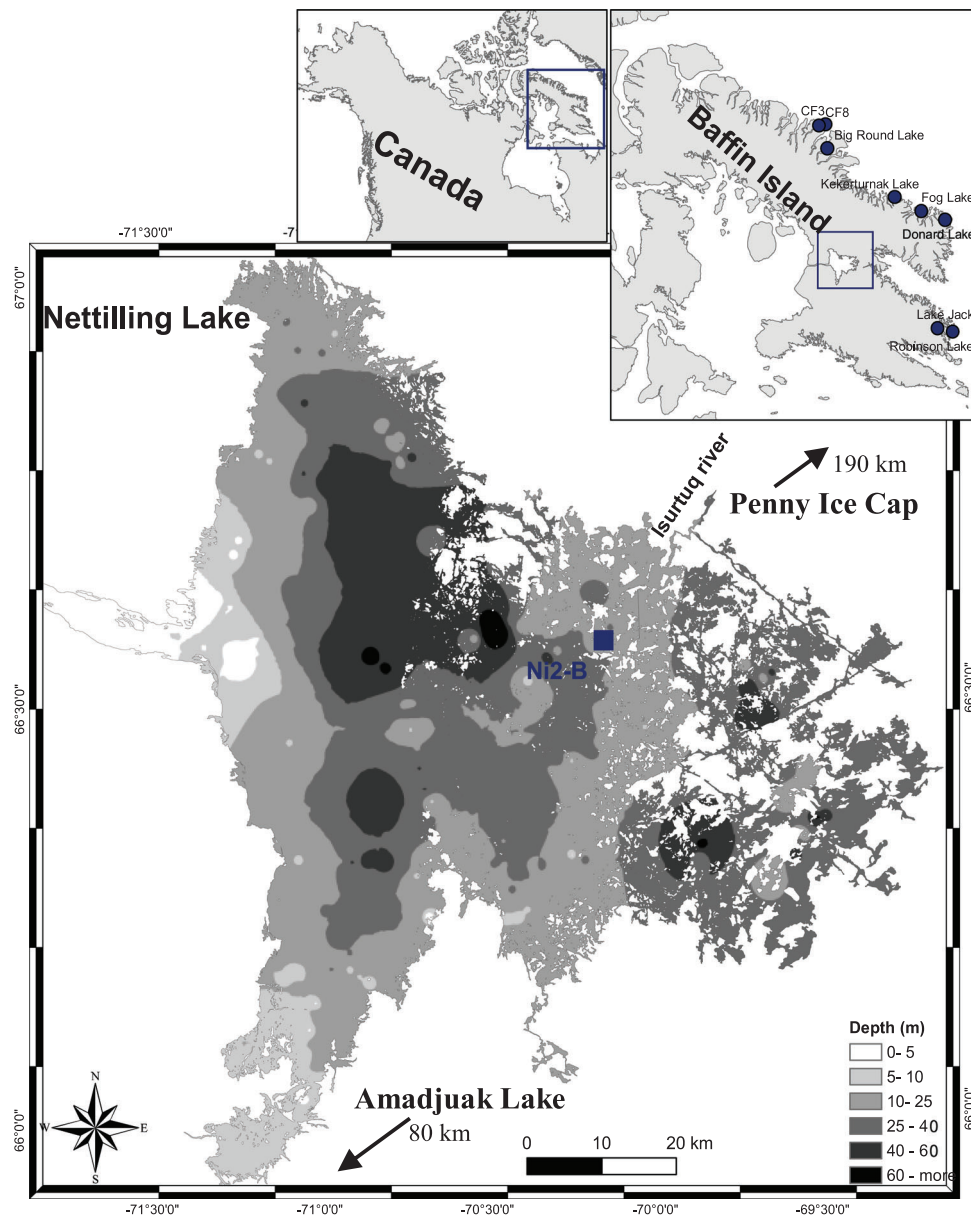


Figure 1. Nettilling Lake bathymetry with Ni2-B coring site location and other Baffin Island lakes (black dots) containing paleoenvironmental data for the past ca. 5000 cal a BP. [Color figure can be viewed at wileyonlinelibrary.com]

model requirements, i.e. species retained represented >1% relative abundance of the assemblages in at least three samples.

Diatom isotope analysis

The upper 35 cm core sample material for isotope analyses ($n=20$; ca. 2 g of dry sediments) was first purified involving chemical (HCl and H_2O_2) and multiple physical (sieving and heavy liquid separation) cleaning steps (Chapligin *et al.*, 2012). Of 20 samples, 13 were already published in Chapligin *et al.* (2016) and seven additional samples were included in this study. Following the purification steps, samples were heated to 1100 °C by ramp degassing under argon flow by inert gas flow dehydration to remove loosely bound oxygen (Chapligin *et al.*, 2010). The samples were then reacted with interhalogen bromine pentafluoride (BrF_5). For this, samples were placed on a nickel plate with holes inside a closed chamber, and then vaporized individually with a CO_2 laser in a BrF_5 atmosphere to quantitatively release O_2 gas from biogenic silica. The oxygen isotope composition was analyzed with an IRMS (PDZ Europa 2020 Mass Spectrometer, Isolab Facility AWI Potsdam) and expressed as $\delta^{18}O$ values relative to VSMOW in per mil (‰).

The $\delta^{18}O$ values were measured against the BFC standard (biogenic material of Burnley diatomite from Shastra County, CA, USA). The measured isotopic composition for BFC within the Nettilling Lake series was $+28.8 \pm 0.04\text{‰}$ ($n=5$; Chapligin *et al.*, 2016). The measured $\delta^{18}O$ was corrected for any remaining contamination using geochemical mass-balancing (for details see Chapligin *et al.*, 2012). The contamination percentage ($Al_2O_3\%$) for each sample was analyzed by energy-dispersive X-ray spectroscopy (EDS) using a scanning electron microscope and calculated by dividing the estimated sample percentage of Al_2O_3 by the 100% contamination Al_2O_3 end-member. Samples showing more than 15% of contamination or >2.5% of Al_2O_3 were discarded (10.5, 18.5 and 25.5 cm).

Results

Age model

The development of an age–depth relationship for the first 35 cm of the core was based on declination correlations between the CALS 10k.1b model output (Korte *et al.*, 2011),

derived mainly from lacustrine sediments and archeological artefacts or volcanic rocks from both hemispheres, and Ni-2B with five tie points (D1–D5) using the AnalySeries 2.0.8 software (Narancic *et al.*, 2021). The derived chronology (Fig. 2c) yielded a mean sedimentation rate of approximately 0.01 cm a^{-1} throughout the freshwater phase (from ca. 5000 to 300 cal a BP).

Diatom assemblage-inferred temperatures

SWT and MAAT reconstructions generated by the diatom-based inference model are presented in Fig. 2 and Table 1. They cover the period ranging from ca. 5000 to 500 cal a BP. The diatom-inferred (DI) SWTs vary between 7.3 and 12.1 °C with associated errors (RMSEP) of ± 0.6 – 1.7 °C, whereas the DI-MAATs vary between -13.1 and -10.1 °C with associated errors (RMSEP) of ± 0.5 – 1.5 °C. The overall average temperatures for the sequence are 9 °C for DI-SWT and -11.6 for DI-MAAT, slightly higher DI-SWT and lower DI-MAAT than modern measured temperatures (7.5 and -10.5 °C; Chaplignin *et al.*, 2016). The results show a slight overall cooling trend with time (since the mid-Holocene) of about 2 °C. Two unusually high DI-SWT values of 12 and 11 °C punctuate the record at 12.50 and 16.50 cm core depth (corresponding to ca. 1360 and 2160 cal a BP, respectively). Because they are so far from the rest of the others, we considered these values questionable and excluded them from further consideration. However, the DI-MAAT values at these depths yielded realistic results, in line with the trend, and were retained.

Diatom isotope composition

The $\delta^{18}\text{O}_{\text{diatom}}$ values of the 19 downcore samples ranged from +24.8 to +21.4‰, with an average of +23.5‰ (Fig. 2; Table 1). Only the diatom sample fraction smaller than $10 \mu\text{m}$ was used and was composed of benthic and planktonic species. The sedimentary $\delta^{18}\text{O}_{\text{diatom}}$ values from 33.5 to 31.5 cm are characterized by increasingly enriched values: from +23.2 to +24.1‰, respectively. This is followed by a sharp decrease to initial values of +23.1‰ at 30.75 cm

(ca. 4400 cal a BP; Fig. 2). Up to 15 cm core depth (ca. 2000 cal a BP), the record shows continuously enriched $\delta^{18}\text{O}_{\text{diatom}}$ values reaching a maximum of +24.8‰ (at 15.25 cm). This is followed by a significant decline from 13.5 to 1.5 cm (ca. 1500–500 cal a BP) ranging between +24.1 and +21.4‰, where the absolute minimum in the $\delta^{18}\text{O}_{\text{diatom}}$ record of +21.4 to +21.5‰ is reached between 4 and 2-cm depth (ca. 800–500 cal a BP). No reliable $\delta^{18}\text{O}_{\text{diatom}}$ values could be obtained for the surface samples, as samples had to be discarded based on contamination assessment criteria ($<2.5\%$ cont. Al_2O_3).

Discussion

The two diatom-based proxies used here to infer summer water temperatures, mean annual air temperatures (diatom assemblages) and hydroclimatic trends ($\delta^{18}\text{O}_{\text{diatom}}$) from ca. 5000 to 500 a BP, showed an overall cooling trend through the Holocene, in line with previous paleoclimatic studies from Baffin Island lakes (Briner *et al.*, 2016).

Diatom assemblage temperature inferences

The models based on the ecological preferences of sedimentary diatom assemblages yielded slightly decreasing temperatures from ca. 4400 to 1200 cal a BP, between the Mid- and Late Holocene. The highest inferred temperatures of the record are observed until ca. 3000 cal a BP, followed by a progressive decline thereafter, which again is in close resemblance with other paleoclimatic regional records (Kerwin *et al.*, 2004). This reflects surface water temperature response to Neoglacial cooling in Nettilling Lake, corresponding to several periods of glacial advances on Baffin Island that reached their Late Holocene maximum between ca. 3000 and 2000 cal a BP (McKay *et al.*, 2018). Further inferred summer cooling continued between ca. 1200 and 800 cal a BP, during what is recognized as the Medieval Climatic Anomaly, a widespread warm phase, albeit with spatial and temporal variability (Wanner *et al.*, 2008; Neukom *et al.*, 2019). Diaz *et al.* (1989)

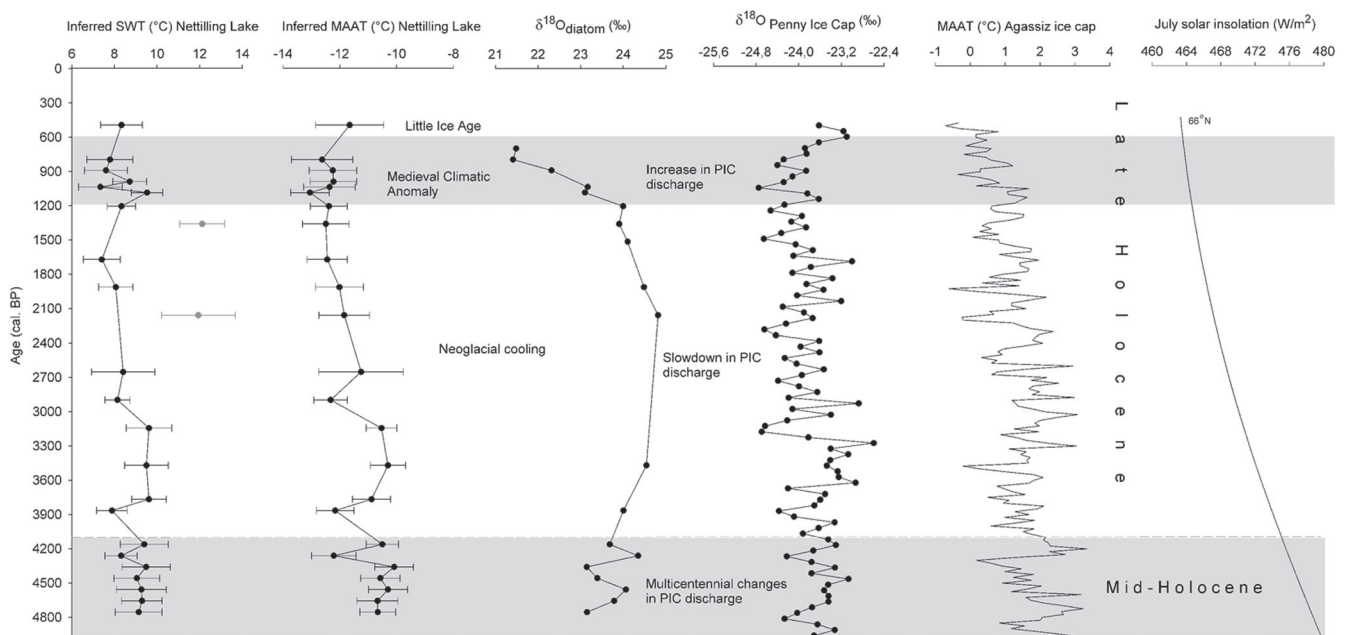


Figure 2. Diatom-inferred summer water temperatures (DI-SWT), mean annual air temperatures (DI-MAAT) and $\delta^{18}\text{O}_{\text{diatom}}$ records plotted against $\delta^{18}\text{O}$ from Penny Ice Cap (PIC; Fisher *et al.*, 1998), MAAT from Agassiz Ice Cap record (Lecavalier *et al.*, 2017), and mean monthly summer solar insolation (Laskar *et al.*, 2004). Globally known warm periods corresponding to the Mid-Holocene and Medieval Climatic Anomaly are marked in gray (Wanner *et al.*, 2008). [Color figure can be viewed at [wileyonlinelibrary.com](https://onlinelibrary.wiley.com)]

Table 1. (a) Diatom-inferred temperatures and (b) contamination percentage correction using energy dispersive X-ray spectroscopy results under scanning-electron microscopy together with measured and corrected $\delta^{18}\text{O}_{\text{diatom}}$ data. DI-SWT (diatom inferred summer water temperatures), DI-MAAT (diatom inferred mean annual air temperatures)

Depth (cm)	Age(cal a BP)	(a)				(b)					
		DI-SWT (°C)	SD DI-SWT	DI-MAAT (°C)	SD DI-MAAT	SiO ₂ (%)	Al ₂ O ₃ (%)	Cont. (%)*	$\delta^{18}\text{O}_{\text{measured}}$ (‰)	$\delta^{18}\text{O}_{\text{corrected}}$ (‰)	$\Delta^{18}\text{O}$ (‰)
0	263										
1	493	8.33	0.98	-11.65	1.20	98.65	0.50	2.40	21.27	21.49	0.22
2	699										
3	747										
4	795	7.79	1.08	-12.62	1.08	99.20	0.23	1.13	21.31	21.41	0.10
5	843										
6	891	7.60	1.01	-12.24	0.84	98.00	0.94	4.56	21.86	22.32	0.46
7	939										
8	988	8.72	0.79	-12.22	0.82	96.16	1.82	8.78	22.21	23.16	0.95
9	1036	7.34	1.03	-12.36	0.91	96.45	1.65	7.97	22.24	23.10	0.86
10	1084	9.53	0.74	-13.05	0.68						
11	1204	8.33	0.67	-12.38	0.65	91.46	1.63	7.88	23.07	24.00	0.92
12	1359	12.12 [†]	1.05	-12.49	0.82	96.74	0.96	4.64	23.37	23.90	0.54
13	1514					97.21	0.60	2.91	23.76	24.10	0.34
14	1515	7.41	0.87	-12.44	0.71	96.19	1.38	6.68	23.67	24.49	0.81
15	1912	8.06	0.81	-12.01	0.84	94.81	2.11	10.20	23.54	24.82	1.28
16	2158	11.94 [†]	1.73	-11.84	0.89						
17	2405										
18	2651	8.41	1.49	-11.25	1.49						
19	2897	8.14	0.59	-12.32	0.59	92.49	2.24	10.81	23.22	24.54	1.32
20	3144	9.62	1.07	-10.53	0.54						
21	3371										
22	3469	9.50	1.03	-10.30	0.62	94.77	2.46	11.90	22.61	24.00	1.39
23	3568										
24	3667										
25	3766	9.62	0.81	-10.88	0.67						
26	3865	7.88	0.72	-12.16	0.66	96.08	1.86	8.99	22.66	23.68	1.02
27	3964										
28	4062										
29	4161	9.40	1.13	-10.50	0.57	95.29	2.39	11.55	22.96	24.35	1.39
30	4260	8.31	0.76	-12.21	0.78	97.99	0.82	3.98	22.71	23.14	0.43
31	4359	9.49	1.13	-10.08	0.68	97.37	1.41	6.80	22.64	23.39	0.75
32	4458	9.05	1.07	-10.57	0.69	97.74	0.89	4.32	23.56	24.06	0.51
33	4557	9.27	1.17	-10.30	0.69	96.42	1.76	8.52	22.81	23.79	0.98
34	4656	9.29	0.95	-10.67	0.72	98.98	0.44	2.14	22.92	23.15	0.23
35	4755	9.14	1.10	-10.66	0.63						

*Data not considered in the reconstruction.

[†]Average for contamination correction: Al₂O₃ 100%cont = 20.7%; $\delta^{18}\text{O}_{100\%cont} = 12.3\text{‰}$ for <10- μm fraction.

and Tamo and Gajewski (2019) document a similar summer cooling trend in reconstructed mean July temperatures based on pollen and tree-ring data from sites across the Canadian Arctic, suggesting intensifying summer cooling in the region from ca. 1000 cal a BP onwards. Based on the surface samples of our core, dated to ca. 500 cal a BP, the DI-SWT at the onset of the Little Ice Age was ca. 8.3 ± 0.3 °C, i.e. 0.8 °C higher than today. This would imply that present-day Nettilling Lake summer temperatures are under greater influence by cold meltwater inputs from the melting PIC than they were 500 years ago.

Despite low sedimentation rates, which can compromise the temporal resolution of the reconstructed temperature trends, there is an overall correspondence between our reconstructed temperatures and the summer temperature trends inferred for Fog Lake by Joynt and Wolfe (2001) using the same model. Inferred temperatures for Nettilling Lake are overall slightly higher than those for Fog Lake, in line with lower present-day summer temperatures in the Arctic Cordillera mountain range where Fog Lake is located (-11.3 °C, Wolfe *et al.*, 2003), than those of the Koukdjuak Plain within the Nettilling Lake catchment basin (-9.1 °C).

This further supports the claim that the diatom-based paleotemperature reconstructions are precise enough to allow for identifications of trends related to natural spatial variability in the climate system of Baffin Island.

$\delta^{18}\text{O}_{\text{diatom}}$ hydroclimatic inferences

Variations in $\delta^{18}\text{O}_{\text{diatom}}$ in lacustrine sediments are mainly controlled by changes in lake water temperature (T_{lake}) and/or lake water isotope composition ($\delta^{18}\text{O}_{\text{lake water}}$) (Leng and Barker, 2006). The $\delta^{18}\text{O}_{\text{lake water}}$, in turn, is influenced by the isotope composition of precipitation ($\delta^{18}\text{O}_{\text{precipitation}}$) and/or lake hydrology (i.e. evaporation, inflow/outflow ratios). Chaplign *et al.* (2016) concluded that T_{lake} at Nettilling Lake has a negligible impact on the $\delta^{18}\text{O}_{\text{diatom}}$ signal, and that the overall $\delta^{18}\text{O}_{\text{diatom}}$ amplitude in the Ni-2B sedimentary record (i.e. including the postglacial marine transgression) of $\Delta^{18}\text{O}$ over 13‰ can be attributed solely to changes in $\delta^{18}\text{O}_{\text{lake water}}$ originating from changes in lake hydrology.

In the lacustrine section of the record, the amplitude of $\delta^{18}\text{O}_{\text{diatom}}$ values is smaller, on the order of $\Delta^{18}\text{O} = 3.4\text{‰}$.

The inferred DI-SWT cooling of 2 °C since the Mid-Holocene would correspond to an isotopic shift of only $\Delta^{18}\text{O} = 0.4\text{‰}$ (Juillet-Leclerc and Labeyrie, 1987; Dodd *et al.*, 2012). Consequently, lake water temperature variations alone cannot explain the change of $\delta^{18}\text{O}_{\text{diatom}}$ values during the last 5000 cal a BP, and therefore other factors, such as changes in the $\delta^{18}\text{O}_{\text{lake}}$, need to be considered.

The regional $\delta^{18}\text{O}_{\text{precipitation}}-T$ relationship of $+0.45\text{‰}/\text{°C}$ (Chapligin *et al.*, 2016) and the 3.4‰ amplitude in the $\delta^{18}\text{O}_{\text{diatom}}$ record since ca. 5000 cal a BP would correspond to a 7.5 °C change in air temperature (assuming this $\delta^{18}\text{O}_{\text{precipitation}}-T$ relationship has remained constant over time). This is higher than expected, especially as these T_{air} -related changes are partly counterbalanced by T_{lake} changes. This reconstruction therefore updates Chapligin *et al.* (2016) who inferred air temperature changes of only 4 °C. We conclude that there must be one or more additional hydrological factors that can explain this amplitude in the sedimentary $\delta^{18}\text{O}_{\text{diatom}}$ record, especially the strong isotopic shift observed between ca. 2000 and 700 cal a BP (Fig. 2). Variable inflow rates of isotopically depleted meltwaters from the PIC are probable drivers of these isotopic changes, as the glaciers associated with the PIC today retreated northwards to their current position and size after the Mid-Holocene lake formation. We therefore suggest that changes in $\delta^{18}\text{O}_{\text{lake water}}$ represent the most important control on the $\delta^{18}\text{O}_{\text{diatom}}$ record, and that they are driven by a combination of T_{air} and hydroclimatic variations of meltwater influx from the PIC.

An increased influx of isotopically depleted glacier meltwater adds water with inherently lower isotopic composition to the lake, which in turn lowers the $\delta^{18}\text{O}_{\text{diatom}}$ signal that reflects the isotopic composition of the ambient water at the time of diatom frustule formation. According to the inferred recent isotope hydrology (Chapligin *et al.*, 2016), the Ni-2B site has one of the lowest lake water isotope compositions (-18.7‰ ; Nettilling Lake min, max and average lake isotope compositions are -19.1 , -16.4 and -17.4‰ , respectively) of Nettilling Lake, reflecting the isotopically depleted inflow via the Isurtuq River. While we cannot estimate the relative importance of meltwater inputs from our results, we nevertheless presume that variations in PIC meltwater inputs are responsible for Isurtuq River discharge changes. Thus, during warmer periods (Mid-Holocene and late Medieval Climatic Anomaly) Isurtuq River discharge increased due to higher glacial meltwater inputs and resulted in slightly depleted $\delta^{18}\text{O}_{\text{diatom}}$ values, while decreases in meltwater inputs and river discharge during the Neoglacial cooling period resulted in reduced influx and therefore slightly enriched $\delta^{18}\text{O}_{\text{diatom}}$ values (Fig. 2). Similar isotopic trends related to varying glacial meltwater influx were recorded in a lake in Kamchatka (Meyer *et al.*, 2015), as well as in ice-proximal marine environments, such as Southern Ocean waters related to Antarctic fluctuations in ice-derived meltwater (Shemesh *et al.*, 1994). This proximity to a prominent, well-constrained meltwater source makes Nettilling Lake an excellent candidate for future studies where paleoclimatological inferences (e.g. temperature, hydrology) based on $\delta^{18}\text{O}_{\text{diatom}}$ records from lacustrine environments can be derived despite the absence of carbonaceous materials.

When compared to the inferred MAAT record from the Agassiz Ice Cap on Ellesmere Island (Lecavalier *et al.*, 2017), and computed mean monthly solar insolation for July and August at 66°N (Laskar *et al.*, 2004), our DI-SWTs, DI-MAATs and $\delta^{18}\text{O}_{\text{diatom}}$ values follow the common regional climatic shifts regulated by decreasing high-latitude summer insolation (Fig. 2). Inferred progressive cooling is also evident from the PIC isotope record (Fig. 2; Fisher *et al.*, 1998). The highest and lowest $\delta^{18}\text{O}_{\text{PIC}}$ values occurred during the Mid-Holocene and

the Neoglacial cooling period, respectively. Lower values in the $\delta^{18}\text{O}_{\text{diatom}}$ record were associated with higher values in $\delta^{18}\text{O}_{\text{PIC}}$ throughout the record. However, this trend is more evident in the upper sediments from 1200 cal a BP onwards. The timing of maximum and minimum $\delta^{18}\text{O}_{\text{PIC}}$ values in core Ni-2B is in line with our hypothesis that increasing and decreasing inputs of isotopically depleted meltwaters from PIC melt associated with regional air temperature changes have a first-order influence on the regulation of the lake water isotope composition at the coring position. Furthermore, Narancic *et al.* (2021) found that planktonic and tychoplanktonic diatoms living in the photic zone were more abundant before Neoglacial cooling, from ca. 5000 to 3000 and from ca. 1200 cal a BP onwards, respectively, when the lake had higher meltwater inputs and water turbidity, while Neoglacial cooling, during which there were less glacial meltwater inputs and lower water turbidity, favored the proliferation of benthic species. Therefore, temperature reconstructions inferred from diatom assemblages combined with $\delta^{18}\text{O}_{\text{diatom}}$ records have proven to be useful in disentangling temperature and climatically driven hydrological signals and have thus contributed to the challenge of separating the specific influence of temperature changes on diatom assemblages from other environmental variables. Despite chronological limitations due to low sedimentation rates, our results have shown both warmer and colder phases at millennial timescales during the Holocene. Combining these two diatom-based proxies in paleoreconstructions is promising.

Potential of diatoms as paleoclimatic indicators/proxies in northern regions

Here, we have shown the possibility of combining two diatom-based climatic proxies in a high-latitude oligotrophic lake subjected to minimal direct anthropogenic influence to reconstruct Late Holocene hydroclimatic changes. The well-defined modern catchment hydrology of the study lake was instrumental in interpreting the isotopic data and should be considered essential in any study using this approach.

The integration of these two proxies is desirable to derive paleoclimatic information for those environments where other proxies are scarce. The combination of the two diatom-based proxies can also help to overcome uncertainties associated with each method. Diatom assemblages may be affected by processes such as inter/intraspecies competition, predation, dissolution and taxonomic evolution. Quantitative reconstructions may also be dependent on the mathematical uncertainties associated with specific transfer functions (Telford *et al.*, 2005), the degree of fit between the modern and sedimentary data sets and taxonomic differences resulting from the interpretations of different analysts. In addition, $\delta^{18}\text{O}_{\text{diatom}}$ may yield certain imprecisions with respect to sample purity. Their combination in this study has revealed that sedimentary diatoms are reliable indicators of past temperature and hydrology changes in the context of high-latitude large oligotrophic lakes, and that in this specific setting, additional information on hydrological processes within the lake watershed can be gained from $\delta^{18}\text{O}_{\text{diatom}}$. In other paleostudies of northern lakes without any glacial meltwater input, such as Lake El'gygytyn in Chukotka (Siberia), $\delta^{18}\text{O}_{\text{diatom}}$ was successfully used as an indicator for MAAT on millennial timescales (Chapligin *et al.*, 2012).

Conclusions

The two diatom-based proxy approaches used in this study yielded an overall decreasing trend in temperatures at Nettilling Lake, Baffin Island, inferred through DI-SWT,

DI-MAAT and $\delta^{18}\text{O}_{\text{diatom}}$ between ca. 5000 and 500 cal a BP. This corresponds to solar insolation changes and is concurrent with previously published paleoclimatic investigations from the region. Our study demonstrates the great potential of combining records based on diatom assemblages and $\delta^{18}\text{O}_{\text{diatom}}$ to reconstruct and disentangle paleoclimatic signals related to air temperature from those related to hydrological changes. Further advances regarding the methodological development (e.g. contamination assessment) and a better understanding of local constraints on $\delta^{18}\text{O}_{\text{diatom}}$, together with detailed specific diatom ecological preferences, will provide an improved understanding of paleoclimatic information inferred from diatom-based lacustrine sedimentary records.

Supporting information

Additional supporting information can be found in the online version of this article.

Figure S1 Photographs of the excessive suspended solid concentrations within the lake's plume region, together with the photograph of the highly turbid Isurtuq River inflow to the lake (photos: Biljana Narancic, August 2014).

Acknowledgements. We thank A. P. Wolfe for sharing the Baffin Island model data with us. The authors would like to thank Ilona Burghardt from the German Research Center for Geosciences (GFZ) for their SEM and EDX support, as well as Quentin Beauvais and Marie-Pier St-Onge from ISMER-UQAR for their help in the laboratory. Additional thanks to Mikaela Weiner from AWI and Claudia Zimmermann and Denis Sarrazin from CEN for their help in the laboratory and in the field. This work was supported through Natural Sciences and Engineering Research Council of Canada Discovery (04743-2017), Northern Supplement (305489-2017) and Polar Continental Shelf Program (646-17 and 635-18) grants awarded to R. Pienitz, and an FRQNT postdoctoral scholarship awarded to B. Narancic. The authors declare no conflict of interest.

Data Availability Statement

The dataset has been submitted to PANGAEA. de and is under the curation process. Please contact the authors of that study for any requests, in the meantime. The dataset from Joynt and Wolfe (2001) is not publicly available.

Abbreviations. DI, diatom-inferred; LIS, Laurentide Ice Sheet; MAAT, mean annual air temperature; PIC, Penny Ice Cap; SWT, surface water temperature.

References

- Bailey HL, Kaufman DS, Sloane HJ *et al.* 2018. Holocene atmospheric circulation in the central North Pacific: a new terrestrial diatom and $\delta^{18}\text{O}$ dataset from the Aleutian Islands. *Quaternary Science Reviews* **194**: 27–38. <https://doi.org/10.1016/j.quascirev.2018.06.027>
- Beaudoin A, Pienitz R, Francus P *et al.* 2016. Palaeoenvironmental history of the last six centuries in the Nettilling Lake area (Baffin Island, Canada): a multi-proxy analysis. *Holocene* **26**: 1835–1846. <https://doi.org/10.1177/0959683616645937>
- Briner JP, McKay NP, Axford Y *et al.* 2016. Holocene climate change in Arctic Canada and Greenland. *Quaternary Science Reviews* **147**: 340–364. <https://doi.org/10.1016/j.quascirev.2016.02.010>
- Cartier R, Sylvestre F, Pailless C *et al.* 2019. Diatom-oxygen isotope record from high-altitude Lake Petit (2200 m a.s.l.) in the Mediterranean Alps: shedding light on a climatic pulse at 4.2 ka. *Climate of the Past* **15**: 253–263. <https://doi.org/10.5194/cp-15-253-2019>
- Chapligin B, Meyer H, Bryan A *et al.* 2012. Assessment of purification and contamination correction methods for analysing the oxygen isotope composition from biogenic silica. *Chemical Geology* **300–301**: 185–199. <https://doi.org/10.1016/j.chemgeo.2012.01.004>
- Chapligin B, Meyer H, Friedrichsen H *et al.* 2010. A high-performance, safer and semi-automated approach for the $\delta^{18}\text{O}$ analysis of diatom silica and new methods for removing exchangeable oxygen. *Rapid Communications in Mass Spectrometry* **24**: 3567–3577. <https://doi.org/10.1002/rcm.4689>
- Chapligin B, Narancic B, Meyer H *et al.* 2016. Paleo-environmental gateways in the eastern Canadian arctic – recent isotope hydrology and diatom oxygen isotopes from Nettilling Lake, Baffin Island, Canada. *Quaternary Science Reviews* **147**: 379–390. <https://doi.org/10.1016/j.quascirev.2016.03.028>
- Crump SE, Young NE, Miller GH *et al.* 2020. Glacier expansion on Baffin Island during Early Holocene cold reversals. *Quaternary Science Reviews* **241**: 106419.
- Diaz HF, Andrews JT, Short SK. 1989. Climatic variations in northern North America (6,000 BP to present) reconstructed from pollen and tree-ring data. *Arctic Alpine Research* **21**: 45–59.
- Dodd JP, Sharp ZD, Fawcett PJ *et al.* 2012. Rapid post-mortem maturation of diatom silica oxygen isotope values. *Geochemistry, Geophysics, Geosystems* **13**: Q09014. <https://doi.org/10.1029/2011GC004019>
- Fisher DA, Koerner RM, Bourgeois JC *et al.* 1998. Penny ice Cap cores, Baffin Island, Canada, and the Wisconsin Foxe Dome connection: two states of Hudson Bay ice cover. *Science* **279**: 692–695. <https://doi.org/10.1126/science.279.5351.692> [PubMed: 9445472]
- Goldenberg Vilar A, Donders T, Cvetkoska A *et al.* 2018. Seasonality modulates the predictive skills of diatom based salinity transfer functions. *PLoS ONE* **13**: e0199343. <https://doi.org/10.1371/journal.pone.0199343> [PubMed: 30458002]
- Gushulak CAC, Laird KR, Bennett JR *et al.* 2017. Water depth is a strong driver of intra-lake diatom distributions in a small boreal lake. *Journal of Paleolimnology* **58**: 231–241. <https://doi.org/10.1007/s10933-017-9974-y>
- Huang S, Herzschuh U, Pstryakova LA *et al.* 2020. Genetic and morphologic determination of diatom community composition in surface sediments from glacial and thermokarst lakes in the Siberian Arctic. *Journal of Paleolimnology* **64**: 225–242. <https://doi.org/10.1007/s10933-020-00133-1>
- Jacques O, Bouchard F, MacDonald LA *et al.* 2016. Distribution and diversity of diatom assemblages in surficial sediments of shallow lakes in Wapusk National Park (Manitoba, Canada) region of the Hudson Bay Lowlands. *Ecology and Evolution* **6**: 4526–4540. <https://doi.org/10.1002/ece3.2179> [PubMed: 27386094]
- Joynt EH, Wolfe AP. 2001. Paleoenvironmental inference models from sediment diatom assemblages in Baffin Island lakes (Nunavut, Canada) and reconstruction of summer water temperature. *Canadian Journal of Fisheries and Aquatic Sciences* **58**: 1222–1243. <https://doi.org/10.1139/f01-071>
- Juggins S. 2013. Quantitative reconstructions in paleolimnology: new paradigm or sick science. *Quaternary Science Reviews*, **64**, 20–32. <https://doi.org/10.1016/j.quascirev.2012.12.014>
- Kerwin MW, Overpeck JT, Webb RS *et al.* 2004. Pollen-based summer temperature reconstructions for the eastern Canadian boreal forest, subarctic, and Arctic. *Quaternary Science Reviews* **23**: 1901–1924.
- Korte M, Constable C, Donadini F *et al.* 2011. Reconstructing the Holocene geomagnetic field. *Earth and Planetary Science Letters* **312**: 497–505. <https://doi.org/10.1016/j.epsl.2011.10.031>
- Kostrova SS, Meyer H, Bailey HL *et al.* 2019. Holocene hydrological variability of Lake Ladoga, northwest Russia, as inferred from diatom oxygen isotopes. *Boreas* **48**: 361–376. <https://doi.org/10.1111/bor.12385>
- Laskar J, Robutel P, Joutel F *et al.* 2004. A long-term numerical solution for the insolation quantities of the Earth. *Astronomy and Astrophysics* **428**: 261–285. <https://doi.org/10.1051/0004-6361:20041335>
- Lecavalier BS, Fisher DA, Milne GA *et al.* 2017. High Arctic Holocene temperature record from the Agassiz ice cap and Greenland ice sheet evolution. *Proceedings of the National Academy of Sciences of the United States of America* **114**: 5952–5957. <https://doi.org/10.1073/pnas.1616287114> [PubMed: 28512225]
- Leclerc AJ, Labeyrie L. 1987. Temperature dependence of the oxygen isotopic fractionation between diatom silica and water. *Earth and Planetary Science Letters* **84**: 69–74. [https://doi.org/10.1016/0012-821X\(87\)90177-4](https://doi.org/10.1016/0012-821X(87)90177-4)

- Leng MJ, Barker PA. 2006. A review of the oxygen isotope composition of lacustrine diatom silica for palaeoclimate reconstruction. *Earth-Science Reviews* **75**: 5–27.
- Maslennikova AV. 2020. Development and application of an electrical conductivity transfer function, using diatoms from lakes in the Urals, Russia. *Journal of Paleolimnology* **63**: 129–146. <https://doi.org/10.1007/s10933-019-00106-z>
- McKay NP, Kaufman DS, Routson CC *et al.* 2018. The onset and rate of Holocene Neoglacial cooling in the Arctic. *Geophysical Research Letters* **45**: 12,487–12,496. <https://doi.org/10.1029/2018GL079773>
- Meyer H, Chaplign B, Hoff U *et al.* 2015. Oxygen isotope composition of diatoms as Late Holocene climate proxy at Two-Yurts Lake, Central Kamchatka, Russia. *Global and Planetary Change* **134**: 118–128. <https://doi.org/10.1016/j.gloplacha.2014.04.008>
- Miller GH, Geirsdóttir À, Zhong Y *et al.* 2012. Abrupt onset of the Little Ice Age triggered by volcanism and sustained by sea-ice/ocean feedbacks. *Geophysics Research Letters* **39**: L02708.
- Narancic B, Pienitz R, Chaplign B *et al.* 2016. Postglacial environmental succession of Nettilling Lake (Baffin Island, Canadian Arctic) inferred from biogeochemical and microfossil proxies. *Quaternary Science Reviews* **147**: 391–405.
- Narancic B, Saulnier-Talbot É, St-Onge G *et al.* 2021. Diatom sedimentary assemblages and Holocene pH reconstruction from the Canadian Arctic Archipelago's largest lake. *Écoscience* 1–14. <https://doi.org/10.1080/11956860.2021.1926642>
- Neukom R, Steiger N, Gómez-Navarro JJ *et al.* 2019. No evidence for globally coherent warm and cold periods over the preindustrial Common Era. *Nature* **571**: 550–554. <https://doi.org/10.1038/s41586-019-1401-2> [PubMed: 31341300]
- Palagushkina O, Wetterich S, Biskaborn BK *et al.* 2017. Diatom records and tephra mineralogy in pingo deposits of Seward Peninsula, Alaska. *Palaeogeography, Palaeoclimatology, Palaeoecology* **479**: 1–15. <https://doi.org/10.1016/j.palaeo.2017.04.006>
- Pienitz R, Smol JP, Birks HJB. 1995. Assessment of freshwater diatoms as quantitative indicators of past climatic change in the Yukon and Northwest Territories, Canada. *Journal of Paleolimnology* **13**: 21–49. <https://doi.org/10.1007/BF00678109>
- Quesada B, Sylvestre F, Vimeux F *et al.* 2015. Impact of Bolivian paleolake evaporation on the $\delta^{18}\text{O}$ of the Andean glaciers during the last deglaciation (18.5–11.7 ka): diatom-inferred $\delta^{18}\text{O}$ values and hydro-isotopic modeling. *Quaternary Science Reviews* **120**: 93–106. <https://doi.org/10.1016/j.quascirev.2015.04.022>
- Reavie ED, Cai M. 2019. Consideration of species-specific diatom indicators of anthropogenic stress in the Great Lakes. *PLoS ONE* **14**: e0210927. <https://doi.org/10.1371/journal.pone.0210927> [PubMed: 31048847]
- Rodríguez-Alcalá O, Blanco S, García-Girón J *et al.* 2020. Large-scale geographical and environmental drivers of shallow lake diatom metacommunities across Europe. *Science of the Total Environment* **707**: 135887. <https://doi.org/10.1016/j.scitotenv.2019.135887>
- Rühland KM, Paterson AM, Smol JP. 2015. Lake diatom responses to warming: reviewing the evidence. *Journal of Paleolimnology* **54**: 1–35. <https://doi.org/10.1007/s10933-015-9837-3>
- Saulnier-Talbot É. 2016. Paleolimnology as a tool to achieve environmental sustainability in the Anthropocene: an overview. *Geosciences* **6**: 26. <https://doi.org/10.3390/geosciences6020026>
- Scherer RR. 1994. A new method for the determination of absolute abundance of diatoms and other silt-sized sedimentary particles—*Journal of Paleolimnology*, **12**, 171. 179. <https://doi.org/10.1007/BF00678093>
- Shemesh A, Burckle LH, Hays JD. 1994. Meltwater input to the Southern Ocean during the Last Glacial Maximum. *Science* **266**: 1542–1544. <https://doi.org/10.1126/science.266.5190.1542> [PubMed: 17841714]
- Smol JP, Birks HJB, Last WM. 2001. *Tracking Environmental Change Using Lake Sediments Volume 3: Terrestrial, Algal, and Siliceous Indicators*. Kluwer Academic Publishers: Dordrecht.
- Sui F, Zang S, Fan Y *et al.* 2020. Establishment of a diatom-total phosphorus transfer function for lakes on the Songnen Plain in northeast China. *Journal of Oceanology and Limnology*. **38**: 1771–1786. <https://doi.org/10.1007/s00343-019-9223-5>
- Swann GEA, Mackay AW, Vologina E *et al.* 2018. Lake Baikal isotope records of Holocene Central Asian precipitation. *Quaternary Science Reviews* **189**: 210–222. <https://doi.org/10.1016/j.quascirev.2018.04.013>
- Tamo C, Gajewski K. 2019. Environmental changes of the last 1000 years on Prince of Wales Island, Nunavut, Canada. *Arctic and Alpine Research* **51**: 348–365.
- Telford RJ, Birks HJ. 2005. The secret assumption of transfer functions: Problems with spatial autocorrelation in evaluating model performance. *Quaternary Science Reviews* **24**: 20–21. <https://doi.org/10.1016/j.quascirev.2005.05.001>
- Wanner H, Beer J, Bütikofer J *et al.* 2008. Mid- to Late Holocene climate change: an overview. *Quaternary Science Reviews* **27**: 1791–1828. <https://doi.org/10.1016/j.quascirev.2008.06.013>
- Wolfe AP. 2003. Diatom community responses to late Holocene climatic variability: a comparison of numerical methods. *Holocene*, **13**, 29–37. <https://doi.org/10.1191/0959683603hl592rp>